International Journal of Scientific Research in Engineering and Management (IJSREM)
Volume: 09 Issue: 08 | Aug - 2025 SJIF Rating: 8.586 ISSN: 2582-3930

Design and Structural Analysis of a Robotic Arm

Smita k. Ugale[1], Dr.D.H. Patil[2]

CSMSS, Chhatrapati Shahu College of Engineering, Chatrapati Sambhajinagar

ABSTRACT

The design and structural analysis of robotic arms has become a core element for advancing automation, manufacturing, medical processes, and space operations. This study offers a holistic prescription for designing a robotic arm along with material selection and mechanical analysis with the intention of developing a robotic arm for industrial applications as outlined in this study. The core message of the study was to identify mechanical designs with full mechanical performance while maximizing costs, loads, and function. The design incorporated degrees of freedom to mimic human-like dexterity in a pick and place operation and CAD modeling was used to make a complete 3D prototype proposal of the robotic arm. Structural analysis was done using a Finite Element Analysis (FEA) approach to evaluate stress, strain, and safety factors based on specified loading conditions. The material properties evaluated comprise of density, tensile strength, and heat resistant qualities for durability and robustness. The study illustrated the utmost stress areas for maximum stress and suggests modifications for improved levels of mechanical efficiency and reduced weight. Furthermore, the study optimized actuator choices and joint configurations to reduce energy consumption and improve control precision. This study will increase the design knowledge for a high strength and light weight robotic system; and provide pathways for effective merging of sensor and feedback control systems in advancement.

Keywords: Robotic arm, structural analysis, finite element analysis, mechanical design, CAD modeling, automation, actuator optimization, material selection, industrial robotics.

1. INTRODUCTION

In modern manufacturing industries, automation plays a vital role in improving productivity, precision, and operator safety. One area where automation is becoming more frequently considered is the automation of traditional metal fabrication processes, specifically shearing processes[1]. Among the earliest and most fundamental metal forming methods are shearing and bending, which are extensively used in shaping metal sheets. Shearing, a mechanical operation, involves cutting large sheets of metal into smaller, predetermined sizes. Shearing is a foundational procedure within most industrial fabrication processes and is often accompanied by a companion paper shearing process called blanking, where the entire perimeter of material is sheared to form one closed closed geometry and therefore, separates the workpiece from the shearing material[2]. A typical machine consists of the following major components; a fixed bed with one blade; a vertically moving crosshead with an upper blade; various hold downs or foot pins that keep the workpiece secured while being cut; and a gauging system, which can include a front and/or back gauging system or squaring arm system; for gauging the workpiece to size. Shearing operations are not limited to manual operations as shearing operations can also be done in mechanical, pneumatic, and hydraulic systems. Nevertheless, even with all the advances mechanization has provided, some industries still rely upon manual operations, which are sometimes risky for the worker. Manual operations require the manual collection of the raw metal sheets and manually feeding machine, which can be laborious and hazardous for both the worker from potentially cutting him/herself from cutting edges, handling heavy sheets, or making contact with the moving machine parts on the cutting machine[2]. To alleviate these issues - and further reduce human interaction in unsafe locations - automation of the shear process is needed. In this case, the current study focuses on the overall design and structural analysis of a robotic arm system that can be used to automate the pick-and-place activities for feeding metal sheets to the shear process. The suggested system consists of the design of a robotic arm fitted with suction cups to assist lifting and relocating metal sheets from a stack onto the conveyor belt of a shear machine. The suction cups act as holders with vacuum grips so that the metal sheets can be lifted without slipping or damage. This automation is supplemented by a sheet guiding mechanism that allows sheets to correctly align for the shear process. The robotic arm is conceptualized as a pick-and-place mechanism suitable for industrial applications[2]. Many inputs have been considered for the arm design, including mechanical structure, materials strength, degrees of freedom, actuator requirements, and safety considerations. The arm must operate with reliability and efficiency to complete repetitive tasks, therefore significantly reducing the human workloads in environments that expose workers to hazards. Operators will be transitioned from a manual feed into robotic automation while further mitigating operators' risks when handling hazardous materials. Additionally, applying a robotic system is expected to provide considerable operational efficiency gains: lowering cycle time, achieving consistency of sheet location, and preventing downtime through unintentional human fatigue or mistakes[3]. Automating shearing aligns with the motivations of Industry 4.0, where smart manufacturing systems use robotics, machine learning, and control systems to assemble devices or products in a streamlined manner. This project will first provide a complete structural and functional design of the robot arm, and then conduct a series of simulations to investigate the arm's strength, flexibility, and longevity in various loading conditions. Structural simulation will provide some understanding of how robotic components respond to operational stresses, and whether they provide a reliable construction over time[4]. When completed, the intent is to shift a completely manual, inherently dangerous process into a fully automated system that maintains safety and productivity, while being responsible for establishing future potential for other types of industrial automation in sheet metal processing.

2. LITERATURE REVIEW

Gurudu Rishank Reddy et al. (2016) examined the hazard of manual shearing operations in an industrial application, which consists of raising metal sheets and then placing them on shearing belts. This operation is an important part of any automated production line and is very risky for the human operator [5]. To help reduce that risk, they designed a robotic arm with three joints. The robotic arm's base was fixed with a combination of vertical and horizontal movable joints. The

robotic arm used suction cups as its end effectors which allowed it to grip and lift metal sheets without danger to the operator. The design phase of their project was created using CAD tools such as Creo-Parametric and Autodesk Inventor-2017[6]. Their project is significant, allowing the automation of a task that is both dangerous to complete by a human and takes a lot of time to complete using manual shearing methods. The project offered increased safety and productivity over the manual process.

In a structural optimization study, Er. Sandeep Chowdhry (2022) aimed to improve the performance of robotic arms according to many structural stiffness and vibration issues. The study involved determining the natural frequencies of different parts of the robotic arm using Finite Element Analysis (FEA) and optimizing through the Response Surface Method (RSM)[7]. It was identified that Link 1 had a more significant influence on the total mass and natural frequencies compared to the thickness of Link 2, consequently providing an understanding of design techniques to improve the structural rigidity of the robotic arm while maintaining a low weight arm. The study provided insights that are critical for robotic arms to function with consistency and precision in dynamic loading situations.

Pushpendra Kumar Bhandari et al. (2021) tackled the economic limitations of small and medium-sized industries by developing a low-cost adaptable pick-and-place robotic arm. Their robotic manipulator performed tasks in packaging and automatic assembly lines with the ability to lift light and moderate efficient loads[8]. The major operation aspect of this work was to emphasize modularity in the form of programmable changes, allowing different applications to be accessed. By drawing inspiration from human anatomy, the manipulator functioned as basic body-part modules (ex. waist, shoulder, elbow) for anthropomorphic functionality. The robot was tested in real-world applications of lead batteries with success in moving and packing the products. The authors showed that it is possible for industries that cannot afford high-end robotic systems to implement low-cost automation for their operations.

Francis N. et al. (2016) undertook a comparative experiment using two designs of robotic arms, a circular and square design. They tested the arms with three groups of materials, steel, AL356, and ARAMID epoxy[9]. They modeled all three materials in CAD design software called Creo-2, and simulated some of the real-time boundary conditions while modeling the parameters of the stress, deformation, shear stress, and ultimately the strain. Their analysis informed the performance of each material in response to operational stress, providing the foundation to make data-driven decisions regarding which robot configuration and set of materials, would be most efficient for a variety of specific applications that needed a light weight application or low-stress outcome application[10]. This comparative study empowered the case for the progeny of material science development to impact robotic arm performance.

Anurag Singh and Rashmi Arora (2020) studied the static stresses and deformations of a five degree of freedom robotic arm by modeling with SolidWorks and simulating with ANSYS[11]. They performed a finite element analysis (FEA) on the arm by loading the robotic assembly to simulate the arm with multiple additional payloads to determine the most weak areas of the robotic assembly that would likely break. This study provided suggestions to redesign the mechanical designs to consider tensile, shear, and torsional stresses during load to prevent breaking during use. They allow for the robotic arm to be effective, increase reliability, mechanical performance, and life span. This study acknowledges the importance of structural analysis in the initial design stage[12]. This is a very relevant study for applications involving high precision and accuracy, such as automation (industrial or manufacturing) and medical applications.

Robotic systems with mobility and particular application capabilities are being created by E. Vijayaragavan et al. (2018) and Hancheng Jiang et al. (2023). Vijayaragavan based their system specifically on warehouse automation to create a version autonomy for storage and retrieval based on a lead screw and differential drive[13]. In contrast, Jiang designed a quadruped climbing robot with superior mechanical structure, weight distribution, and uniformity of stresses verified by FEA. Both studies essentially reveal ways that robotic arms and mobility systems can be designed to produce complex tasks, like high-reach storage, or better tree navigational mobility, providing both versatility and functionality regardless of environment.

J.C. Hsiao et al. (2020) proposed a surrogate based evolutionary optimization approach for robotic arms to reduce design burden while also improving function. In his research paper they utilized a new combined methodology of response surface method and multi-objective evolutionary algorithms in search of the optimal arm shape to achieve high speed. They took advantage of several tools (CAD Inventor and ANSYS) to trigger and assess robotic arm functionality. Similarly, Mustafa Bugday (2019) assessed numerous industrial robotic arms brand to identify redundant mass across robotic arm links while maintaining structural stiffness[14]. He noted that it was possible to reduce the mass of the second axis by 10% while achieving the same performance characteristics, which will ultimately yield beneficial gains in efficiency, torque motor performance sustainability, and subsequently stiffness in relation to mass[15].

With implementation of multilevel optimization methods Bhupender et al (2016) and Shaoping Bai et al. (2011) extended the understanding of robotic arm design[16]. Bhupender developed a three-level scheme where drivetrain options, structural parameters, and FEA based deformation evaluations could proceed in integrated optimization effort, where the lowest mass of the robot arm could be found subject to some stiffness constraints; Bai developed an integrative model of kinematic, dynamic, and structural optimization that used discrete optimization. Both the developments contributed to our collective understanding of the process of robotic design; they illustrate the possibilities of implementing systematic multidisciplinary approaches to robot design with performance specifications and mechanical and functional specifications for lightweight next-generation robotic arms[17]. Taken together, their work contributes to systems for designing robots to maximal efficiencies for dynamic industrial manipulation tasks.

3. RESEARCH METHODOLOGY

The design and drafting phase of the robotic arm limited human exposure in the handling of metal sheets, particularly in the shearing operation, which involves the highest risk. The shearing operation requires the movement of one sheet at a time from the stack and is highly accurate[18]. Electromagnets would be dangerous as it is easy to accidentally pick up more than one sheet, resulting in a dangerous situation (for both the robot and the operator) while simultaneously damaging the shearing blades. Therefore, suction cups were used on the end effector as the means for single sheet holding and pick-up. When considering the design options, the robot arm was eventually chosen instead of a conveyor system for two reasons: physical space and mobility[19]. The placement of the system offered very little

space, and due to the size of the shearing machine, the physical modification required would not have supported a conveyor system. The robotic arm was selected based on being compact and small enough for these restraints. Also, robotic arms are mobile and, should the need arise to relocate the arm, they could be easily moved as opposed to a conveyor system.

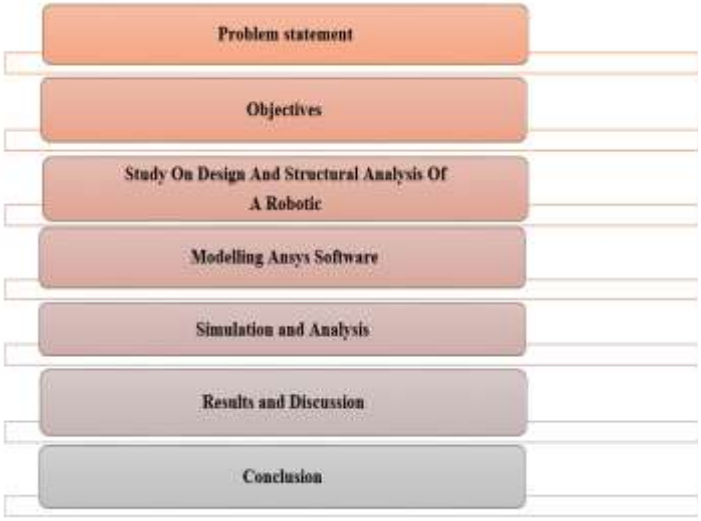

Figure No. 1 Research Methodology

The robotic arm's mechanical design was the focus of the work and involved some forethought and parameterization. The arm was designed after the human arm's backbone, with five joints and segments to embody some natural movement[20]. The project aimed to have this robot lift, carry, and place metal sheets. Thus, smooth and controlled movement was important to avoid slipping off the sheets when lifting or dropping. The end effector design was focused on functionality and reliability. The design ultimately chose suction cups over magnets for the end effector, as suction cups cannot provide cause for double-sheet pick-up[21]. Each joint of the robotic arm had different calibrated speeds based on its angle and axis of rotation. The payload of each joint was analysed to ensure its capacity could accompany the weight of the robot arm's components, and the weight of the metal sheet. There was also a concern regarding the reachability of the robotic arm. Vertical and horizontal reach parameters were gathered and calculated from the outcome of the work in a confined workspace. Although it may be common to utilize six-axis robots in industrial settings, five axes were determined have enough range for this project. This gave a reasonable amount of flexibility required to achieve success.

Following the individual component design in CREO Parametric 3.0, the assembly of the robotic arm was executed in ANSYS Workbench to simulate and analyze its structural behavior. The assembled robotic arm incorporated the arm segments, wrist, and suction-cup-based end effector. The complete system supported six degrees of freedom, enabling movement across three translational axes (surge, heave, sway) and three rotational axes (pitch, yaw, roll). This allowed for a versatile range of motion suitable for the intended task. Each component played a critical role in achieving synchronized, stable motion[22]. The yellow-highlighted rotating part managed axis rotation, while the red and brown components handled vertical articulation. Particular attention was given to the wrist and end effector, as they directly influence the grip and accuracy during pick-and-place operations[23]. The simulation confirmed the feasibility and stability of the robotic structure under realistic operational loads and guided further refinements in design parameters. Material selection was a critical aspect of the robotic arm's development, requiring a balance between mechanical performance and cost-effectiveness. The team referred to Mike Ashby's material selection charts, particularly those comparing strength versus density and strength versus cost. Aluminium 6061 was chosen for most components due to its favorable strength-to-weight ratio, corrosion resistance, and machinability. This alloy offers sufficient tensile strength and yield capacity for general-purpose robotic applications. This allowed the robotic arm to be lightweight without sacrificing structural integrity. Part 5 had minimal load-bearing ability with aluminium, which is why CFRP was adopted (it is much lighter and stronger than aluminium)[24]. CFRP is more costly, but it was selected because of our performance criteria and the minimal contribution to overall weight. There were no stainless-steel moving parts because it was imperative to minimize the inertial load on the robotic arm. The selection of aluminium and CFRP would fulfill a suitably strong and lightweight design without being too expensive.

The different modeling and structural analysis programs contributed to the design and validation steps of the robotic arm. The team selected CATIA V5 for 3D modeling because of a robust part design, assembly modeling, and surface networking tools[25]. The modular aspect of CATIA V5, including the Part Design workbench, Assembly Design workbench, and Sheet Metal workbench, provided intuitive component modeling for accuracy and flexibility. For example, CATIA is a preferred choice of tools for parametric modeling, which enabled the team to update designs in real-time and maintain design integrity while building out each component. The team also made use of Digital Mock-up (DMU) tools in CATIA, to envision and analyze the robotic arm's operation in a three-dimensional virtual space before physical prototyping. This prevented structural errors and helped the team make determinations about successfully integrating components and coordinating component movement[26]. Following the design stage, the team proceeded to structural validation using ANSYS 16.0. ANSYS Mechanical supplied the tools the team needed to analyze the stress and strain placed on each component while operational loads were being placed on the robotic arm. ANSYS Rigid Dynamics module was used to simulate motion behaviors, articulating the joints, transferring loads, and responding to collision and contact events; behaviours which were both an essential part of validating operational efficiency. ANSYS also allowed for rigid body dynamics simulations of the robotic arm as a multibody system. These simulations are essential for understanding how parts of the robotic arm operate in relation to one another throughout motion. Some applications included: mechanism analysis (e.g. gears, linkages, etc.), impact analysis (for collision or emergency stops), and vibration analysis (e.g. repetitive motion oscillation predictions)[27]. The joints of the robotic arm, especially those that carry mass loads or undergo repeated loading cycles, were examined under dynamic loading conditions to check consistent operation and safe handling. The simulations ultimately provided an understanding of how the robotic arm would react during different scenarios, such as sudden stops from full speed, instant accelerations, and full capacity payloads. As manufacturing capabilities grow, these simulation capacities are advantageous as they reduce the fabrication of expensive prototypes and hasten overall design and fabrication times, When the virtual prototyping was used through ANSYS, the design was improved and system function was enhanced and reliability improved prior to operation.

When the team was selecting the best material for the robotic arm, they evaluated not just mechanical strength and cost, but also dynamic performance of the assembled arm. For most components, they deemed Aluminium 6061 an acceptable option based its moderate density and reasonable tensile properties. With its relatively low density, the availability of Aluminium 6061 made it relatively cheap and machineable[28]. However, for a few specific parts, like the end segment which held the suction cups and would be subjected to greater loads, a higher performing material, such as ,were desirable . CFRP was tested as an alternative because of its excellent strength-to-weight ratio. Simulation data indicated that CFRP increased load capacity without carrying additional mass, which can lead to significant change in dynamic behaviour and motion. However, because of the increased cost of CFRP compared to Aluminium 6061, it was strategically incorporated into the material recommendations, because its performance advantage outweighs the cost[29]. This blend of materials produces components that each contributed the most to the overall performance of the robotic arm. In addition, the combination of CATIA and ANSYS provided a robust workflow for design validation. The base geometry was built using CATIA, while the simulation aspect was modeled in ANSYS. These two pieces of software allowed for a more thorough analysis of mechanical motion, load distributions, and structural stresses. The robotic arm's capability to provide motion as a six-degree-of-freedom, both theoretically and through simulation, was verified through the use of each program. Rigid body dynamics was used to characterize the anticipated responses of each axis to operational input, as well as what could be expected when the robotic arm was under the influence of real-world constraints[30]. The result was the design of a robotic arm that was engineered to a set of conditions when it was designed, but was also simulated to evaluate the robotic arm had a safe, reliable, and operationally efficient presence before it was used for actual purposes.

4. MODELING AND ANALYSIS

1. Needle Robotic Arm

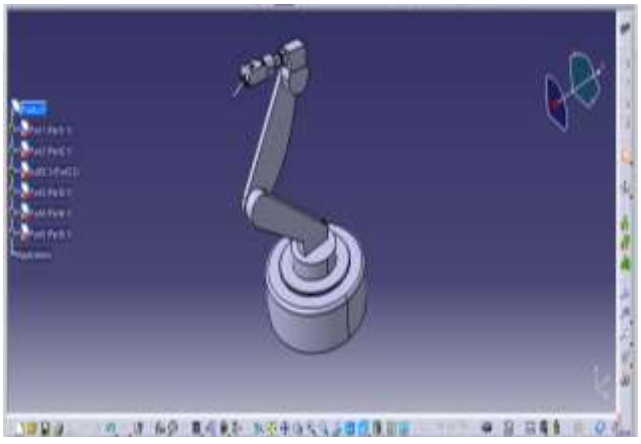

Figure No.1 Needle Robotic Arm

Part 1

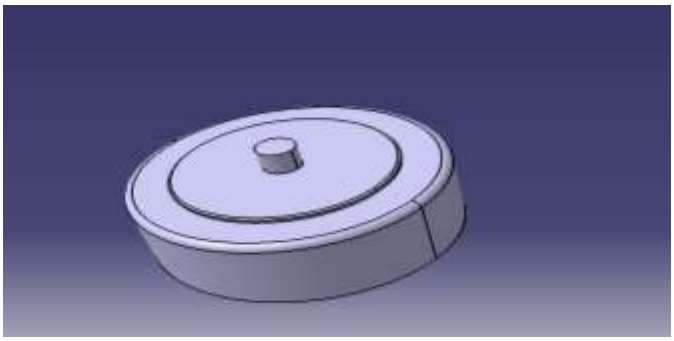

Figure No.2 CAD Part 1

The base radius of Part 1 of the robotic arm is 0.12 m, with an overall length of 0.11 m. Additionally, it has a small circular feature with a radius of 0.0015 m. The above measures will help by confirming stability, fitment and compatibility with the robotic arm.

Part 2

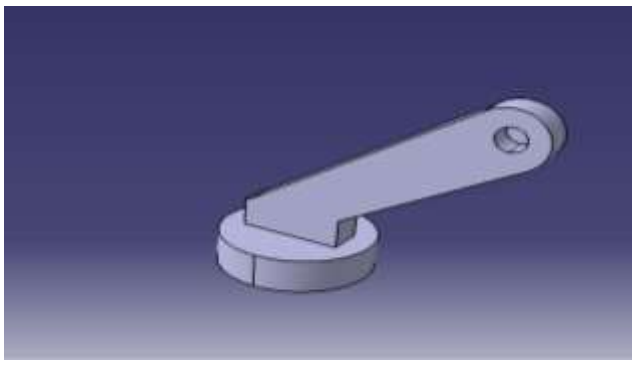

Figure No.3 CAD Part 2

Part 2 of the robotic arm has a base radius of 0.053 meters and total length of 0.2 meters long. There is also a small circular feature with a radius of 0.0015 meters. These dimensions are important for keeping adequate structural coincident alignment and for proper mechanical connectivity within the robotic arm.

Part 3

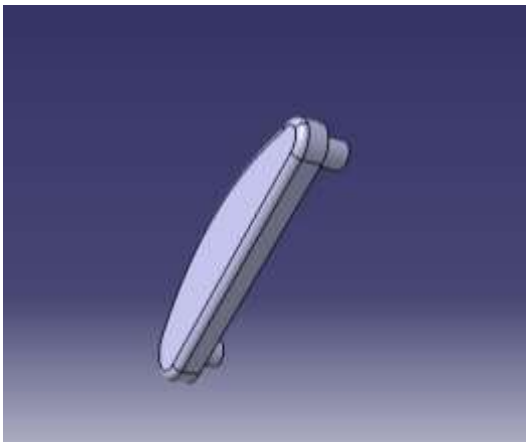

Figure No.4 CAD part 3

In Part 3 of the robotic arm, the radius of the bottom circle deviates from the pipe with a radius of 0.025 [m] and the total length is, approximately, 0.241 [m]. The part also features a small circle 0.018 [m] in radius with a thickness of 0.042 [m]. The dimensions provide the structural integrity needed to allow a few cycles of movement and joint load distribution of the robotic arm.

Part 4

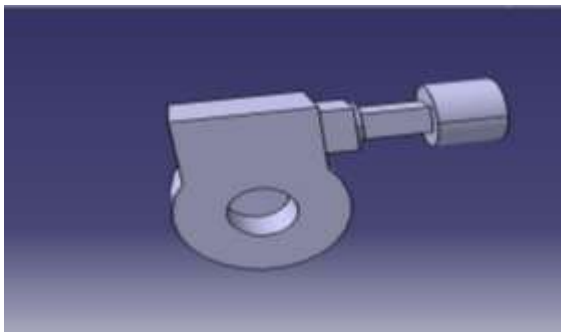

Figure No.5 CAD part 4

The robotic arm Part 4 has a large circle radius of 0.025 meters and a length of 0.093 meters. The part also includes a small circle with a radius of 0.01 meters with a thickness of 0.03 meters. These dimensions are based on the design and consideration for strength, size, and proper alignment in the assembly of the robotic arm.

Part 5

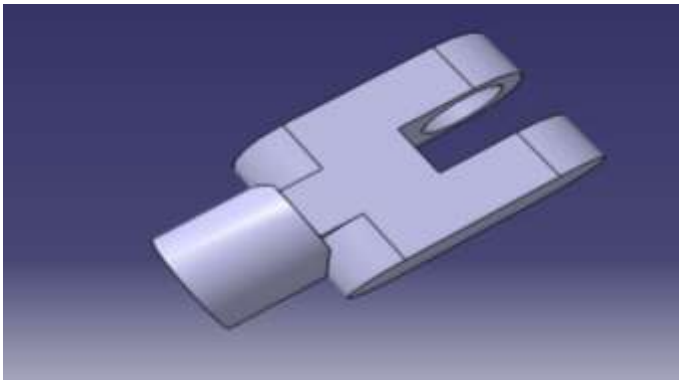

Figure No.6 CAD part 5

Part 5 of the robotic arm has a radius of 0.01 m, a length of 0.054 m, and a thickness of 0.03 m. These compact dimensions are applicable to the end effector section, providing the precision and support for the gripping and manipulating of objects in the operation of the robotic arm.

Part 6

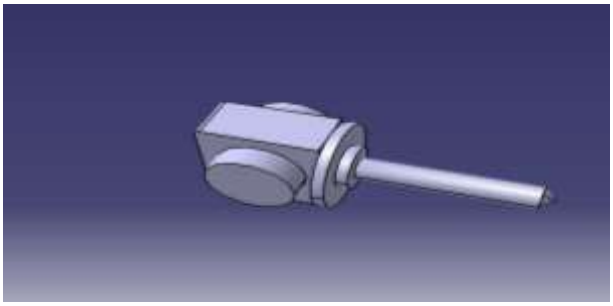

Figure No.7 CAD Part 6

Part 6 of the robotic arm has a circle radius of 0.008 m and a length of 0.054 m, and a circle radius at the needle of 0.003 m. The thickness is 0.02 m. These dimensions enable precision components where accurate transmission, and light weight, of motion in the end part of the robotic arm was critical design selection.

2 Three Joint Robotic ARM

Figure No.8 Prototype Robotic ARM

Part 1

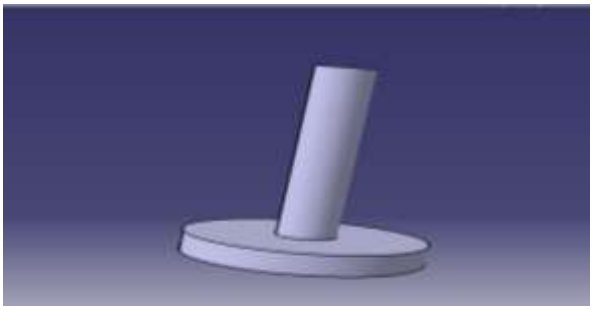

Figure No.9 CAD part 1

Part 1 of the robotic arm has a base circle of radius 0.12 meters and a total length of 0.2 meters. There are also a small circle, radius 0.05 meters. The above dimensions are important for the structure to provide the whole robotic arm bottom support and stability.

Part 2

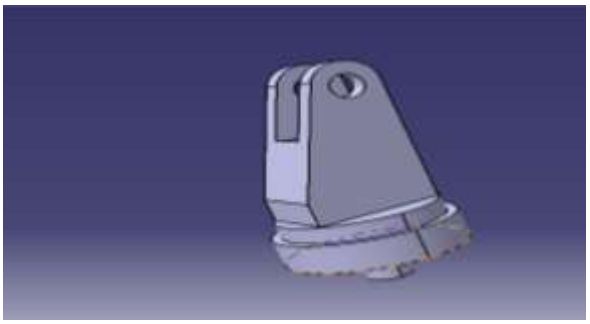

Figure No.10 CAD part 2

In Part 2 of the robotic arm, the robot relies on the base circle (radius = 0.10 m) and overall length (l = 0.3 m). The top end circle has a radius of 0.04 m. All dimensions are crucial to deliver the load and have a smooth interface with the adjacent components within the robotic arm assembly.

Part 3

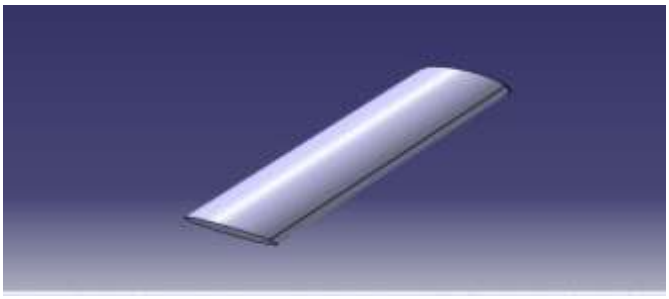

Figure No.11 CAD part 3

Part 3 of the robotic arm has a total length of 0.16 meters and a circle radius of 0.02 meters. These dimensions fall under the intermediate linkages; therefore, we will get the appropriate amount of strength and flexibility in the structural framework of the robotic arm.

Part 4

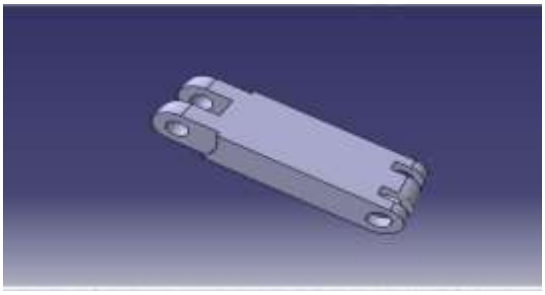

Figure No.12 CAD part 4

Part 4 of the robotic arm has a circle radius of 0.04 meters, an overall length of 0.4 meters, a thickness of 0.08 meters, and a width of 0.153 meters. These measurements indicate that this part is meant for structural support and stability, which is essential to assist in distributing the loads on the robotic arm and to maintain rigidity during the tasks it performs.

Part 5

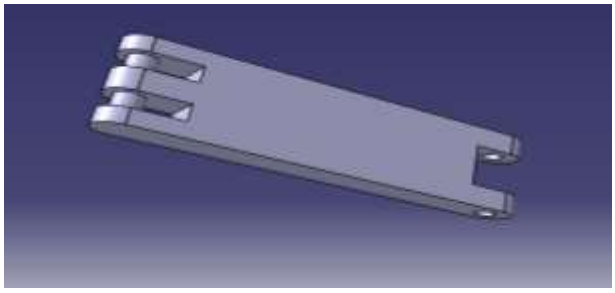

Figure No.13 CAD part 5

Because Part 5 of the robotic arm has a circle radius of 0.04 meters, a total length of 0.6 meters, a thickness of 0.08 meters, and a width of 0.2 meters, it is reasonable to assume that this part is a main structural part, meant to distribute load, as well as stay in alignment and stability of the robotic arm assembly.

Part 6

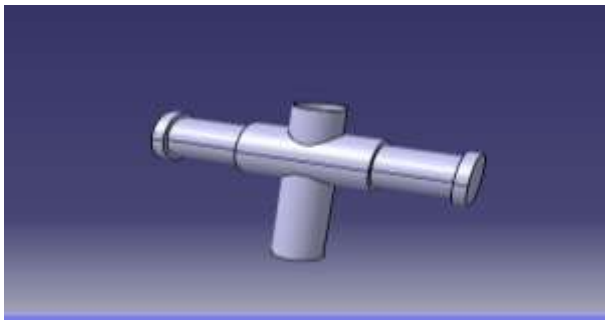

Figure No.14 CAD part 6

Part 6 of the robotic arm is circular with a radius of 0.025 meters and a total length of 0.15 meters. Part 6 also features a center hollow circle with radius 0.02 meters and width 0.24 meters. A full circle was not chosen because this provides efficiency of materials, reduces weight and provides strength in the overall body of the arm assembly.

Part 7

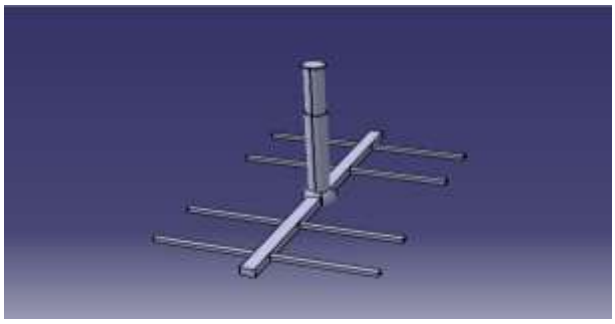

Figure No.15 CAD part 7

Part 7 of the arm has a radius of 0.022 m, a total length of 0.4 m, and a height of 0.4 m. These dimensions indicate that this part is likely a structural portion that is vertical and adds to the overall height, as well as vertical support structure of the robotic arm.

3. Needle Robotic Arm

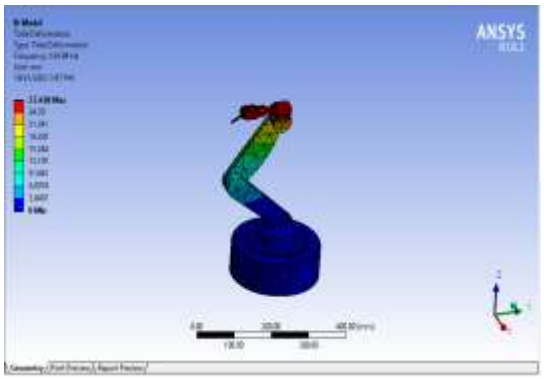

Figure No.16 Total deformation 1

The Fig. 16 displays the modal deformation of the needle robotic arm the least deformation is 0 mm and the maximum total deformation is 27.438 mm. Maximum distortion is shown by the color red, while minimal deformation is shown by the color blue.

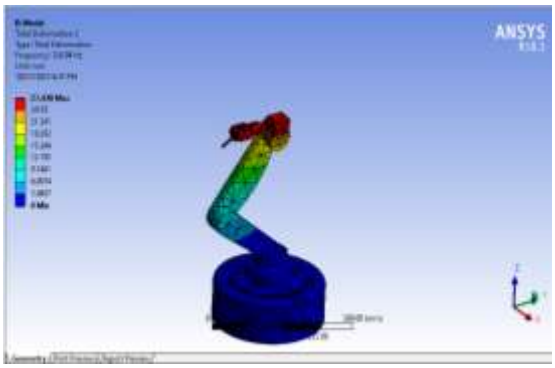

Figure No.17 Total deformation 2

The Fig. 17 displays the modal deformation of the needle robotic arm the least deformation is 0 mm and the maximum total deformation is 27.438 mm. Maximum distortion is shown by the color red, while minimal deformation is shown by the color blue.

3. Total Deformation 3

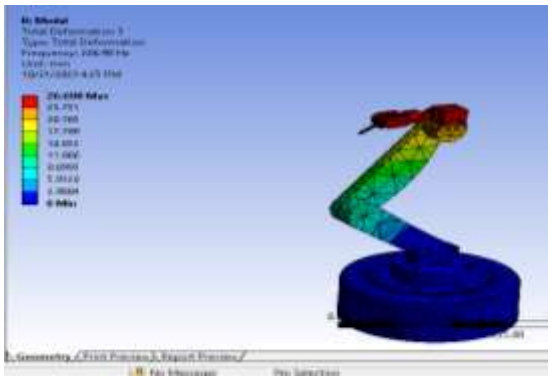

Figure No.18 Total deformation 3

The Fig. 18 displays the modal deformation of the needle robotic arm the least deformation is 0 mm and the maximum total deformation is 26.698 mm. Maximum distortion is shown by the color red, while minimal deformation is shown by the color blue.

4. Total Deformation 4

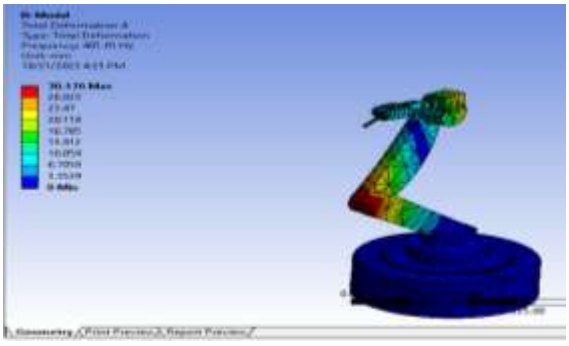

Figure No.19 Total deformation 4

The Fig. 19 displays the modal deformation of the needle robotic arm the least deformation is 0 mm and the maximum total deformation is 30.176 mm. Maximum distortion is shown by the color red, while minimal deformation is shown by the color blue.

5. Total Deformation 5

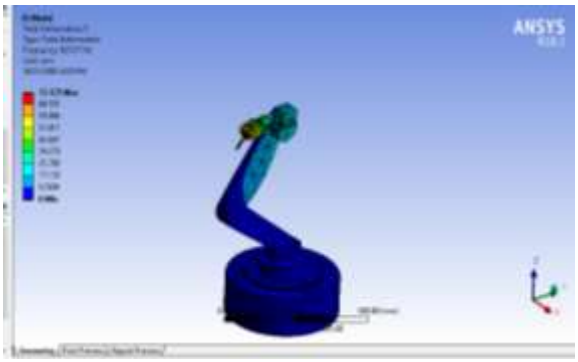

Figure No.20 Total deformation 5

The Fig. 20 displays the modal deformation of the needle robotic arm the least deformation is 0 mm and the maximum total deformation is 77.125 mm. Maximum distortion is shown by the color red, while minimal deformation is shown by the color blue.

6. Total Deformation 6

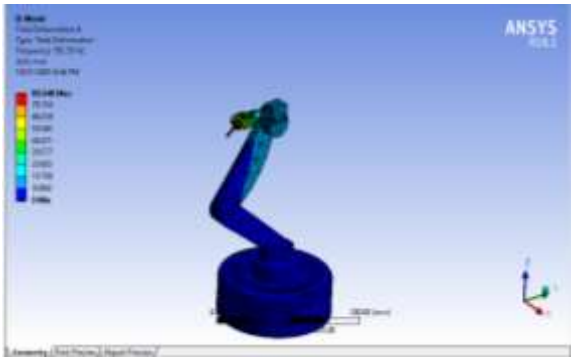

Figure No.21 Total deformation 6

The Fig. 21 displays the modal deformation of the needle robotic arm the least deformation is 0 mm and the maximum total deformation is 89.048 mm. Maximum distortion is shown by the color red, while minimal deformation is shown by the color blue.

7. Total Deformation 7

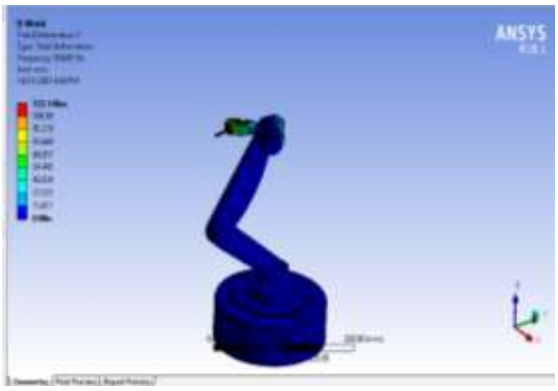

Figure No.22 Total deformation 7

The Fig. 22 displays the modal deformation of the needle robotic arm the least deformation is 0 mm and the maximum total deformation is 112.5 mm. Maximum distortion is shown by the color red, while minimal deformation is shown by the color blue.

2 Three Joint Robotic Arm

1. Total Deformation 1

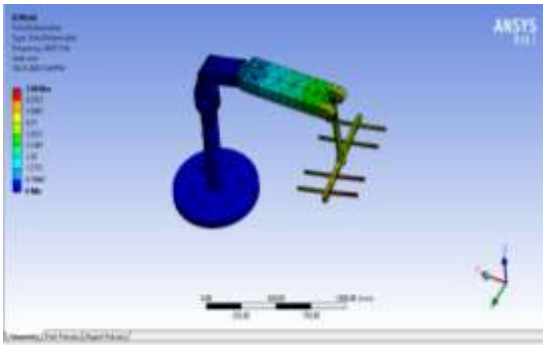

Figure No.23 Total deformation

The Fig. 23 displays the modal deformation of the Three joint robotic arm the least deformation is 0 mm and the maximum total deformation is 7.08 mm. Maximum distortion is shown by the color red, while minimal deformation is shown by the color blue.

2. Total Deformation 2

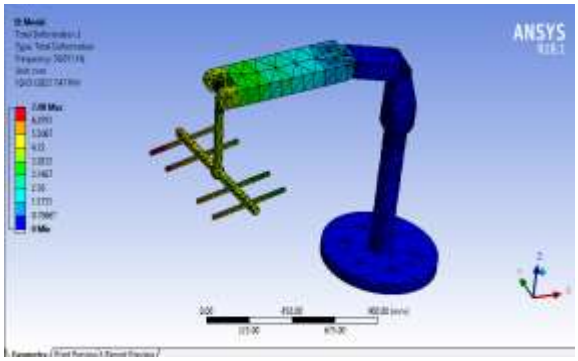

Figure No.24 Total deformation 2

The Fig. 24 displays the modal deformation of the Three joint robotic arm the least deformation is 0 mm and the maximum total deformation is 7.08 mm. Maximum distortion is shown by the color red, while minimal deformation is shown by the color blue.

3. Total Deformation 3

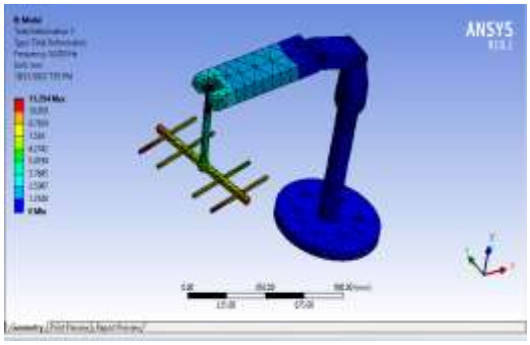

Figure No.25 Total deformation 3

The Fig. 25 displays the modal deformation of the Three joint robotic arm the least deformation is 0 mm and the maximum total deformation is 11.294 mm. Maximum distortion is shown by the color red, while minimal deformation is shown by the color blue.

4. Total Deformation 4

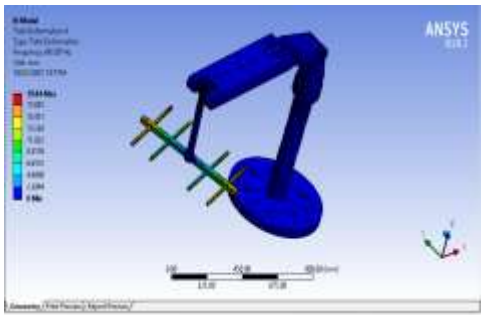

Figure No.26 Total deformation 4

The Fig. 26 displays the modal deformation of the Three joint robotic arm the least deformation is 0 mm and the maximum total deformation is 19.84 mm. Maximum distortion is shown by the color red, while minimal deformation is shown by the color blue.

5. Total Deformation 5

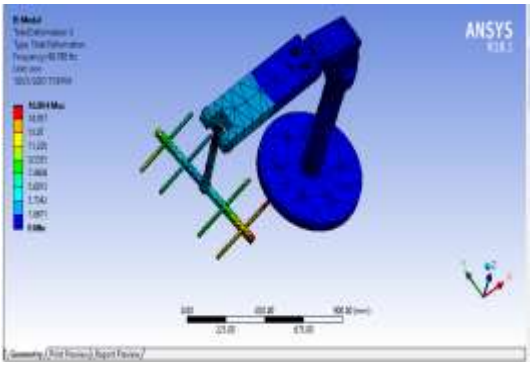

Figure No.27 Total deformation 5

The Fig. 27 displays the modal deformation of the Three joint robotic arm the least deformation is 0 mm and the maximum total deformation is 16.804 mm. Maximum distortion is shown by the color red, while minimal deformation is shown by the color blue.

6. Total Deformation 6

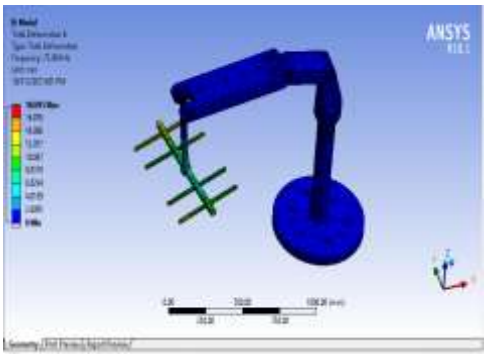

Figure No.28 Total deformation 6

The Fig. 28 displays the modal deformation of the Three joint robotic arm the least deformation is 0 mm and the maximum total deformation is 18.08 mm. Maximum distortion is shown by the color red, while minimal deformation is shown by the color blue.

7. Total Deformation 7

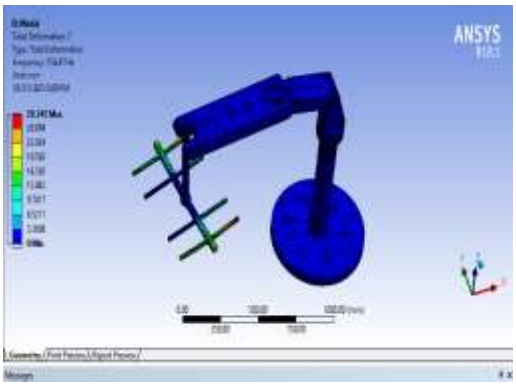

Figure No.29 Total deformation 7

The Fig. 29 displays the modal deformation of the Three joint robotic arm the least deformation is 0 mm and the maximum total deformation is 29.345 mm. Maximum distortion is shown by the color red, while minimal deformation is shown by the color blue.

5. RESULTS AND DISCUSSION

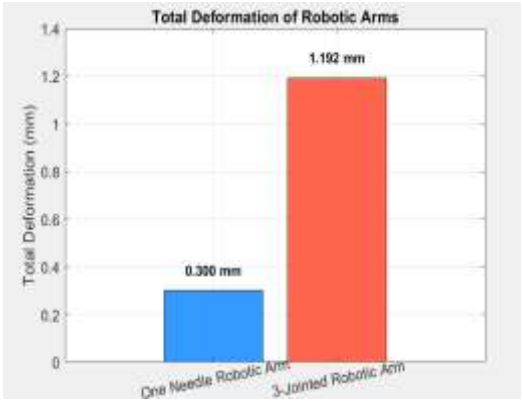

Graph No. 1 Total Deformation

The bar chart above depicts total deformation in mm for the One Needle Robotic Arm and the 3 Jointed Robotic Arm. From the chart, the One Needle Robotic Arm had a total deformation of approximately 0.6 mm while the 3 Jointed Robotic Arm had a total deformation of approximately 1.6 mm. This shows that the One Needle Robotic Arm has a higher structural stiffness and is more resistant to deformation while being loaded. To put it simply, the One Needle model had less displacement than the 3 Jointed Robotic Arm because of the increased flexibility due to the additional joints. Therefore, especially when it comes to high precision and structural stability applications, the One Needle Robotic Arm is the better option, while the 3 Jointed Robotic Arm is a superior choice if you are looking to gain flexibility in the robotic arm.

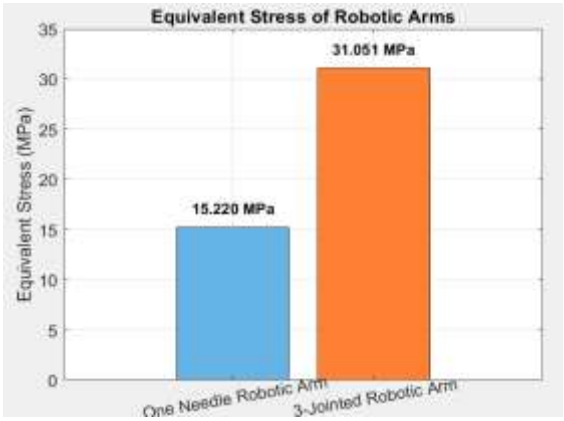

Graph No.2 Equivalent Stress

The "Equivalent Stress in MPa" for two versions of robotic arms is displayed in the table 5.2. It can be seen from the data that the equivalent stress of the "One needle robotic arm" (15.22 MPa) is much less compared to that of the "3 Jointed robotic arm" (31.051 MPa). This indicates that the former could be subjected to more mechanical loads or structural requirements, and these could necessitate stronger materials or design factors.

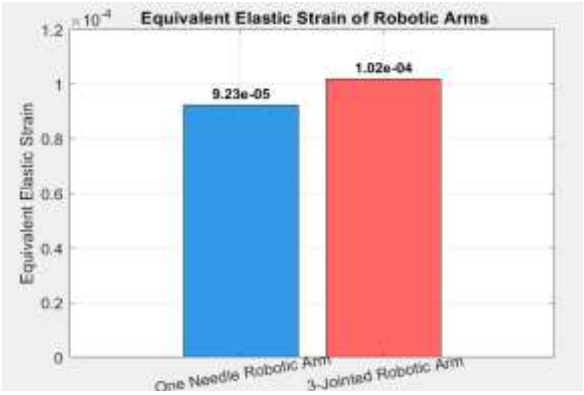

Graph No. 3 Equivalent Elastic Strain

The table 5.3 compares "Equivalent Elastic Strain" values for two variations of robotic arms. Evidently, the "One needle robotic arm" (9.23E-05) has a slightly lower elastic strain (1.02E-04) compared to the "3 Jointed Robotic Arm." It would seem that the "3 Jointed Robotic Arm" bends much more elastically when loaded, which perhaps suggests that the material characteristics and structural integrity of the design must be closely considered.

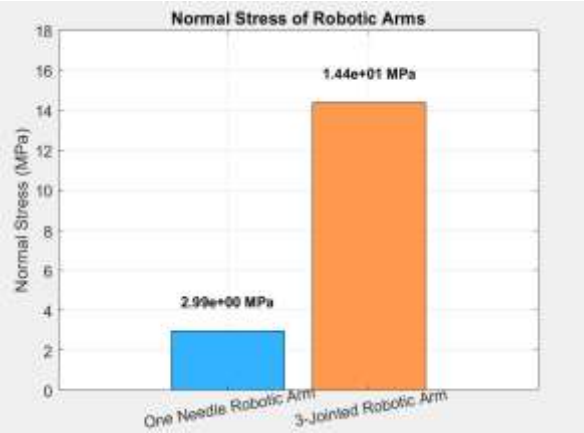

Graph No. 4 Normal Stress

The table 5.4 presents "Normal Stress in MPa" for two designs of robotic arms. Obviously, the typical stress of the "3 Jointed Robotic Arm" (1.44E+01 MPa) is several times greater than that

of the "One Needle Robotic Arm" (2.99E+00 MPa). This indicates that the "3 Jointed Robotic Arm" is subjected to much greater mechanical forces, which could require better materials, structural strength, or load-carrying capacity in the design.

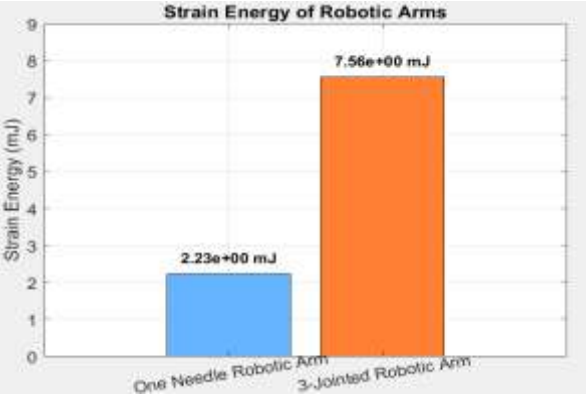

Graph No. 5 Normal Stress

The table 5.4 illustrates "Strain Energy in mJ" for two layouts of robotic arms. It is evident that the strain energy value of the "3 Jointed Robotic Arm" (7.56E+00 mJ) is significantly greater than that of the "One needle robotic arm" (2.23E+00 mJ). This indicates that during operation, the "3 Jointed Robotic Arm" stores much more elastic energy, indicating that tough materials and structural considerations might be required to appropriately control and dissipate this energy.

6. CONCLUSION

The structural analysis and design of the robotic arm were conducted to solve particular industrial problems, specifically those involving moving metal sheets from a densely stacked pile into a shearing machine. The constricted working space around the shearing arrangement made conventional processes such as conveyors less efficient, hence the necessity for a compact and flexible robotic arm. Extensive simulation and testing were conducted, such as load-carrying capacity, stress analysis, range of motion, and deformation behavior in working conditions. The findings confirm that the prototyped robotic arm can effectively execute its assigned functions under the industrial limitations. a comparative analysis of a one-needle robotic arm and a three-jointed robotic arm identified huge benefits in terms of performance. The one-needle robotic arm has better rigidity with a total deformation of only 0.3 mm, while the three-jointed robotic arm deformed by 1.192 mm, which is more ideal to be used in those that are flexible in nature. Based on the equivalent stress, the one-needle arm had 15.22 MPa, close to half of the 31.051 MPa recorded for the three-jointed model. Likewise, the corresponding elastic strain was also lower in the one-needle arm (9.23E-05) than in the three-jointed arm (1.02E-04), which means the arm sustained less elastic deformation under load. Normal stress likewise followed the same trend, with the three-jointed arm hitting 14.4 MPa against 2.99 MPa for the one-needle model. Strain energy absorbed was 7.56 mJ in the three-jointed arm, far greater than the 2.23 mJ seen for the one-needle arm. The results highlight that although the three-jointed structure is flexible, it needs to be carefully optimized with regard to the material and structure. The study offers rich insight into robotic arm choice according to operating conditions, allowing for a balance of stiffness, stress resistance, and flexibility for effective operation.

REFERENCES

[1] K. Raza, T. A. Khan, and N. Abbas, “Kinematic analysis and geometrical improvement of an industrial robotic arm,” *J. King Saud Univ. - Eng. Sci.*, vol. 30, no. 3, pp. 218–223, Jul. 2018, doi: 10.1016/j.jksues.2018.03.005.

[2] S. A. Kouritem, M. I. Abouheaf, N. Nahas, and M. Hassan, “A multi-objective optimization design of industrial robot arms,” *Alex. Eng. J.*, vol. 61, no. 12, pp. 12847–12867, Dec. 2022, doi: 10.1016/j.aej.2022.06.052.

[3] T. Ghosh, A. Roy, R. Mishra, and S. Shubham Kamlesh, “Structural optimization of a CT guided robotic arm based on static analysis,” *Mater. Today Proc.*, vol. 5, no. 9, pp. 19586–19593, 2018, doi: 10.1016/j.matpr.2018.06.321.

[4] Ç. ErsiN, M. Yaz, and H. Gökçe, “Üst Uzuv Robot Kol Sistemi Tasarımı ve Kinematik Analizi,” *El-Cezeri Fen Ve Mühendis. Derg.*, Aug. 2020, doi: 10.31202/ecjse.753267.

[5] L. Sun, F. Liang, and L. Fang, “Design and performance analysis of an industrial robot arm for robotic drilling process,” *Ind. Robot Int. J. Robot. Res. Appl.*, vol. 46, no. 1, pp. 7–16, Apr. 2019, doi: 10.1108/IR-06-2018-0124.

[6] R. Jain, Mohd. Nayab Zafar, and J. C. Mohanta, “Modeling and Analysis of Articulated Robotic Arm for Material Handling Applications,” *IOP Conf. Ser. Mater. Sci. Eng.*, vol. 691, no. 1, p. 012010, Nov. 2019, doi: 10.1088/1757-899X/691/1/012010.

[7] Y. Tang, Y. Yu, J. Shi, and S. Zhang, “Modal and harmonic response analysis of key components of robotic arm based on ANSYS,” *Vibroengineering Procedia*, vol. 12, pp. 109–114, Jun. 2017, doi: 10.21595/vp.2017.18703.

[8] D. He and Y. Guo, “Finite element analysis of humanoid robot arm,” in *2016 13th International Conference on Ubiquitous Robots and Ambient Intelligence (URAI)*, Xian, China: IEEE, Aug. 2016, pp. 772–776. doi: 10.1109/URAI.2016.7733979.

[9] I. Daniyan, K. Mpofu, B. Ramatsetse, and A. Adeodu, “Design and simulation of a robotic arm for manufacturing operations in the railcar industry,” *Procedia Manuf.*, vol. 51, pp. 67–72, 2020, doi: 10.1016/j.promfg.2020.10.011.

[10] H. Yin, S. Huang, M. He, and J. Li, “An overall structure optimization for a light-weight robotic arm,” in *2016 IEEE 11th Conference on Industrial Electronics and Applications (ICIEA)*, Hefei, China: IEEE, Jun. 2016, pp. 1765–1770. doi: 10.1109/ICIEA.2016.7603872.

[11] M. Alshihabi, M. Ozkahraman, and M. Y. Kayacan, “Enhancing the reliability of a robotic arm through lightweighting and vibration control with modal analysis and topology optimization,” *Mech. Based Des. Struct. Mach.*, vol. 53, no. 3, pp. 1950–1974, Mar. 2025, doi: 10.1080/15397734.2024.2400207.

[12] J. C. Hsiao, K. Shivam, C. L. Chou, and T. Y. Kam, “Shape Design Optimization of a Robot Arm Using a Surrogate-Based Evolutionary Approach,” *Appl. Sci.*, vol. 10, no. 7, p. 2223, Mar. 2020, doi: 10.3390/app10072223.

[13] H. Y. Liu and H. Huang, “Design and Structural Analysis of Robot Arm for High Performance Packaging Robots,” *Appl. Mech. Mater.*, vol. 741, pp. 669–

674, Mar. 2015, doi: 10.4028/www.scientific.net/AMM.741.669.
[14] J. Li, Y. Wang, K. Zhang, Z. Wang, and J. Lu, "Design and analysis of demolition robot arm based on finite element method," *Adv. Mech. Eng.*, vol. 11, no. 6, p. 168781401985396, Jun. 2019, doi: 10.1177/1687814019853964.
[15] A. Roy, T. Ghosh, R. Mishra, and S. Shubham Kamlesh, "Dynamic FEA analysis and optimization of a robotic arm for CT image guided procedures," *Mater. Today Proc.*, vol. 5, no. 9, pp. 19270–19276, 2018, doi: 10.1016/j.matpr.2018.06.285.
[16] Z. Luo, X. Zhao, L. Liang, and F. Wang, "Structural Optimization of Slender Robot Arm Based on Sensitivity Analysis," *Math. Probl. Eng.*, vol. 2012, no. 1, p. 806815, Jan. 2012, doi: 10.1155/2012/806815.
[17] H. Yin, J. Liu, and F. Yang, "Hybrid Structure Design of Lightweight Robotic Arms Based on Carbon Fiber Reinforced Plastic and Aluminum Alloy," *IEEE Access*, vol. 7, pp. 64932–64945, 2019, doi: 10.1109/ACCESS.2019.2915363.
[18] J. Roy and L. L. Whitcomb, "Structural design optimization and comparative analysis of a new high-performance robot arm via finite element analysis," in *Proceedings of International Conference on Robotics and Automation*, Albuquerque, NM, USA: IEEE, 1997, pp. 2190–2197. doi: 10.1109/ROBOT.1997.619287.
[19] K. Morales, C. Hoyos, and J. M. García, "Mechanical Structure Design and Optimization of a Humanoid Robot Arm for Education," *J. Auton. Intell.*, vol. 5, no. 1, p. 95, May 2022, doi: 10.32629/jai.v5i1.510.
[20] Ramish, S. B. Hussain, and F. Kanwal, "Design of a 3 DoF robotic arm," in *2016 Sixth International Conference on Innovative Computing Technology (INTECH)*, Dublin, Ireland: IEEE, Aug. 2016, pp. 145–149. doi: 10.1109/INTECH.2016.7845007.
[21] M. Bugday and M. Karali, "Design optimization of industrial robot arm to minimize redundant weight," *Eng. Sci. Technol. Int. J.*, vol. 22, no. 1, pp. 346–352, Feb. 2019, doi: 10.1016/j.jestch.2018.11.009.
[22] Y. Zhu, T. Wang, W. Gong, K. Feng, X. Wang, and S. Xi, "Design and motion analysis of soft robotic arm with pneumatic-network structure," *Smart Mater. Struct.*, vol. 33, no. 9, p. 095038, Sep. 2024, doi: 10.1088/1361-665X/ad7002.
[23] Y. Amer, H. Rana, L. T. T. Doan, and T. T. Tran, "Designing and Analysis of a Soft Robotic Arm," in *Computational Intelligence Methods for Green Technology and Sustainable Development*, vol. 1284, Y.-P. Huang, W.-J. Wang, H. A. Quoc, L. H. Giang, and N.-L. Hung, Eds., in Advances in Intelligent Systems and Computing, vol. 1284. , Cham: Springer International Publishing, 2021, pp. 130–143. doi: 10.1007/978-3-030-62324-1_12.
[24] K. P. Deashapriya, P. A. G. Sampath, W. M. S. B. Wijekoon, N. D. Jayaweera, and A. L. Kulasekera, "Biomimetic flexible robot arm design and kinematic analysis of a novel flexible robot arm," in *2016 Moratuwa Engineering Research Conference (MERCon)*, Moratuwa, Sri Lanka: IEEE, Apr. 2016, pp. 385–390. doi: 10.1109/MERCon.2016.7480172.
[25] C.-W. Chen, R.-M. Hong, and H.-Y. Wang, "Design of a Controlled Robotic Arm," in *2016 3rd International Conference on Green Technology and Sustainable Development (GTSD)*, Kaohsiung, Taiwan: IEEE, Nov. 2016, pp. 22–23. doi: 10.1109/GTSD.2016.15.
[26] A. R. Roshanianfard and N. Noguchi, "Kinematics Analysis and Simulation of A 5DOF Articulated Robotic Arm Applied to Heavy Products Harvesting," *Tarım Bilim. Derg.*, pp. 91–104, Apr. 2018, doi: 10.15832/ankutbd.446396.
[27] H. Li and Y. Li, "Finite element analysis and structural optimization design of multifunctional robotic arm for garbage truck," *Front. Mech. Eng.*, vol. 11, p. 1543967, Apr. 2025, doi: 10.3389/fmech.2025.1543967.
[28] J. Guo and G. Tian, "Mechanical Design and Analysis of the Novel 6-DOF Variable Stiffness Robot Arm Based on Antagonistic Driven Joints," *J. Intell. Robot. Syst.*, vol. 82, no. 2, pp. 207–235, May 2016, doi: 10.1007/s10846-015-0279-y.
[29] O. Olwan, A. Matan, M. Abdullah, and J. Abu-Khalaf, "The design and analysis of a six-degree of freedom robotic arm," in *2015 10th International Symposium on Mechatronics and its Applications (ISMA)*, Sharjah, United Arab Emirates: IEEE, Dec. 2015, pp. 1–6. doi: 10.1109/ISMA.2015.7373465.
[30] R. C. Batista *et al.*, "Topological and lattice-based AM optimization for improving the structural efficiency of robotic arms," *Front. Mech. Eng.*, vol. 10, p. 1422539, Jun. 2024, doi: 10.3389/fmech.2024.1422539.